

NUMERICAL INVESTIGATIONS OF HYDROGEN RELEASE AND DISPERSION DUE TO SILANE DECOMPOSITION IN A VENTILATED CONTAINER

Rocco Rotundo¹, Jianjun Xiao², Thomas Jordan², Daniele Melideo¹, Umberto Desideri¹

¹Department of Energy, Systems, Territory and Construction Engineering, University of Pisa, Pisa 56122, Italy

²Institute of Nuclear Energy Technologies, Karlsruhe Institute of Technology, Karlsruhe 76021, Germany

ABSTRACT

In recent years, new chemical release agents based on silane are being used in the tire industry. Silane is an inorganic chemical compound consisting of a silicon backbone and hydrogen. Silanes can be thermally decomposed into high-purity silicon and hydrogen. If silane is stored and transported in Intermediate Bulk Containers (IBCs) equipped with safety valves in vented semi-confined spaces, such as ISO-Containers, hydrogen can be accumulated and become explosive mixture with air. A conservative CFD analysis using the GASFLOW-MPI code has been carried out to assess the hydrogen risk inside the vented containers. Two types of containers with different natural ventilation systems were investigated under various hypothetical accident scenarios. A continuous release of hydrogen due to the chemical decomposition of silane from IBCs was studied as the reference case. The effect of the safety valves on hydrogen accumulation in the container which results in small pulsed releases of hydrogen was investigated. The external effects of the sun and wind on hydrogen distribution and ventilation were also evaluated. The results can provide detailed information on hydrogen dispersion and mixing within the vented enclosures, and used to evaluate the hydrogen risks, such as flammability. Based on the assumptions used in this study, it indicates that the geometry of ventilation openings plays a key role in the efficiency of the indoor air exchange process. In addition, the use of safety valves makes it possible to reduce the concentration of hydrogen by volume in air compared to the reference case. The effect of the sun, which results in a temperature difference between two container walls, allows a strong mixing of hydrogen and air, which helps to obtain a concentration lower than both the base case and the case of the pulsed releases. But the best results for the venting process are obtained with the wind that can drive the mixture to the downwind wall vent holes.

Keywords: hydrogen dispersion, CFD, safety analysis, ventilated container

1. INTRODUCTION

Nowadays, the increased interest shown in hydrogen and the prospect of having a clean energy carrier has led the scientific community to constantly put more and more resources into studying the safety of hydrogen. One of the most interesting topics is accidental release in confined environments. Hysafe [1] with the HyInside [2] and SUSANA Project [3] has been edited for guidance on the use of hydrogen in confined space [4]. Computational Fluid Dynamics (CFD) can help to predict possible hydrogen release accidents in enclosed spaces. A benchmark was carried out to validate CFD codes for hydrogen release and dispersion in confined and ventilated space in the HyIndoor project [5]. Other studies can be found in the literature with different flow rates, different conditions, and different geometries of the enclosures, including both release and dispersion [6]. In this study, the releases of hydrogen have very particular conditions: a very low mass flow rate at atmospheric pressure and temperature, and releases occur in a really constrained environment.

Occasional hydrogen releases may occur in the chemical decomposition processes of some substances. For example, this may be the case where substances composed of silicon and hydrogen bonds are involved (Hydrogen-Bonded Silicon Compounds) [7]. These substances can be found in various forms, such as emulsions, fluids, elastomers, and resins. For safety reasons, some potential risks in their storage, handling, and use should be considered. Under certain conditions, bonds between hydrogen and silicon can be broken and pure gaseous hydrogen can be released in the surrounding environment. Three conditions must be present for releasing gaseous hydrogen: a source of Si-H bonds, an active hydrogen source, and a catalyst source. In particular, compounds in the form of emulsions can emit hydrogen

continuously because, containing water, they contain an unlimited supply of active hydrogen. Acid or basic emulsions can act as catalysts themselves.

In this analysis, a water-based releasing agent in the form of emulsion that is used in the tire industry was considered. When stored indoors, it can potentially generate enough hydrogen to make the environment flammable, and, without any mitigation measures, it can cause an explosion. The storage tanks that are used in these cases are the so-called Bulk Intermediate Containers (IBCs). For safety reasons, relief valves are used to relieve the internal overpressure caused by gas production inside the IBC, making the release into the surrounding environment periodic (pulsed). Release frequency depends on gas production and valve opening overpressure. IBCs are loaded inside containers, usually 20 ft containers, which can be transported on ships, trains, or trucks. Normally, the companies producing the releasing agents rent the containers, and therefore the available container models have specifications that cannot be changed. The choice of container type is influenced by both safety and economic reasons. The natural ventilation system plays a key role in ensuring air exchange and hydrogen venting. A ventilated container (coffee container) has holes for ventilation both on the top and on the bottom of the long side walls, so that it is theoretically the one that can guarantee efficient ventilation, but it is at least five times more expensive than a standard type of container, known as an ISO (International Organisation for Standardisation), which, however, has milder ventilation, having only four holes of ventilation located on the top of the long side walls.

A CFD numerical analysis was carried out, in order to establish if flammable clouds could form due to the accidental release of hydrogen inside a 20 ft ISO container, in which sixteen IBCs are loaded. The objective is to estimate the amount of hydrogen contained in the container after a period of time, its distribution, and the time required for the hydrogen concentration to reach the lower flammability limit (LFL). The approach in this analysis is conservative, so first a continuous release of hydrogen within the ISO container, equal to the gas released by the emulsions, is considered, and then evaluated the differences with a pulsed release dictated by the operation of the safety valves (more realistic case). In addition, the external effects of the sun and wind were studied. Finally, a continuous releases of hydrogen is tested in the ventilated container.

2. PHYSICAL MODEL

Simulations were performed with the CFD code GASFLOW-MPI (version 3.5), developed at the Karlsruhe Institute of Technologies [8] [9]. It is a well-developed parallel scalable CFD code to predict transport, mixing, and combustion of hydrogen and other gases in nuclear and non-nuclear systems, and it is well validated and used for hydrogen safety analysis. The robust Arbitrary-Lagrangian-Eulerian (ALE) approach in GASFLOW-MPI is used to solve a 3-D time-dependent compressible Navier-Stokes equation system.

In this section, there will be introduced the equations solved by the code [8]: conservation equations and the turbulence model.

2.1 CONSERVATION EQUATIONS

Volume equation

$$\frac{\partial V}{\partial t} = \oint_S \mathbf{b} \cdot \mathbf{A} dS \quad (1)$$

Mixture mass equation

$$\frac{\partial}{\partial t} \int_V \rho dV = \oint_S \rho(\mathbf{b} - \mathbf{u}) \cdot \mathbf{A} dS + \int_V S_\rho dV \quad (2)$$

where ρ is the density of the mixture, \mathbf{u} is the fluid velocity vector, V is the discretized fluid control volume, \mathbf{b} is the velocity vector of the contour surface S , and S_ρ is the mass source term. The term $\mathbf{b} - \mathbf{u}$ is the relative velocity between the control surface and the fluid.

Transport equation for individual species

$$\frac{\partial}{\partial t} \int_V \rho_\alpha dV = \oint_S \rho_\alpha (\mathbf{b} - \mathbf{u}) \cdot \mathbf{A} dS - \oint_S (\mathbf{J}_\alpha \cdot \mathbf{A}) + \int_V S_{\rho,\alpha} dV \quad (3)$$

where α denotes the gas species, ρ_α is the macroscopic density of the species α , $\mathbf{J}_\alpha \cdot \mathbf{A}$ is the mass diffusion flux vector with Cartesian geometry components, and $S_{\rho,\alpha}$ is the source term. $D_{\alpha \rightarrow \text{mix}}$ is the mass diffusion coefficient of species α into the gaseous mixture.

Mixture momentum equations

$$\begin{aligned} \frac{\partial}{\partial t} \int_V \rho \mathbf{u} dV = & \oint_S \rho \mathbf{u} (\mathbf{b} - \mathbf{u}) \cdot \mathbf{A} dS - \oint_S p d\mathbf{S} + \int_V \rho \mathbf{g} dV \\ & - \oint_S (\boldsymbol{\tau} \cdot \mathbf{A}) dS - \oint_S (\mathbf{D}_d \cdot \mathbf{A}) dS + \int_V \mathbf{S}_m dV \end{aligned} \quad (5)$$

where p is the pressure, $\boldsymbol{\tau}$ is the viscous stress tensor, \mathbf{g} is the gravitational vector, \mathbf{D}_d is the internal structure drag tensor, and \mathbf{S}_m is any source term. On the right side the terms are respectively the flux of momentum through the control surface, the sum of the pressure gradient, gravity, viscous forces on the control volume, fluid drag forces acting on structural surfaces, and any additional momentum sources.

Equation of change for total internal energy

$$\frac{\partial}{\partial t} \int_V \rho I dV = \oint_S \rho I (\mathbf{b} - \mathbf{u}) \cdot \mathbf{A} dS - \oint_S p (\mathbf{u} \cdot \mathbf{A}) - \oint_S (\mathbf{q} \cdot \mathbf{A}) dS + \int_V S_I dV \quad (6)$$

where I is the mixture specific internal energy, S_I is the energy source, and \mathbf{q} is the energy flux vector.

2.2 TURBULENCE MODEL

Detached Eddy Simulation (DES) model was used in the simulations [10] [11]. DES is a hybrid technique that can switch between a RANS (Reynolds Average Navier-Stokes) model to a LES (Large Eddy Simulations) model. If the mesh resolution is fine enough to solve the turbulence, the code uses LES, while if not a RANS model is used. In GASFLOW-MPI DES model is based on k - ε model. This model has been validated for GASFLOW-MPI successfully [12].

The turbulent kinetic energy k is determined from solution of its transport equation:

$$\frac{\partial}{\partial t} (\rho k) + \nabla \cdot (\rho k \mathbf{u}) = \nabla \cdot \left[\left(\mu + \frac{\mu_t}{\sigma_k} \right) \nabla k \right] + G_k + G_b - \frac{\rho k^{-\frac{3}{2}}}{l_{\text{des}}} + S_k \quad (12)$$

Where μ_t is the turbulent dynamic viscosity, G_k is turbulent generation due to the viscous forces, G_b turbulence generation due to the buoyancy, and generation from other sources. The rate of dissipation ε , similarly, is determined from the solution of its transport equation.

$$\frac{\partial}{\partial t} (\rho \varepsilon) + \nabla \cdot (\rho \varepsilon \mathbf{u}) = \nabla \cdot \left[\left(\mu + \frac{\mu_t}{\sigma_\varepsilon} \right) \nabla \varepsilon \right] + C_{\varepsilon 1} (G_k + G_b) - \frac{\rho k^{-\frac{3}{2}}}{l_{\text{des}}} + S_\varepsilon \quad (13)$$

l_{des} , l_{rke} , and l_{les} are respectively the length scales of DES model, k - ε model, and LES model, and can be calculated as follow:

$$l_{des} = \min(l_{rke}, l_{les}), \quad l_{rke} = \frac{k^{3/2}}{\varepsilon}, \quad l_{les} = C_{des} \Delta_{max} \quad (14)$$

where $C_{des}=0.65$ is the DES coefficient, and Δ_{max} is biggest cell size.

$$\mu_t = \rho C_\mu \frac{k^2}{\varepsilon} \quad (15)$$

3. SIMULATION MODELLING

The configuration is representative of a container in a free environment, without any other object around it. Inside the container 16 IBCs are loaded with a space between them of 10 cm. The production of gas from a single IBC is set equal to 4 H_2/h . In the simulations, releases of hydrogen from every IBC take place from four cells on the top with a total area of $10cm^2$, both for a continuous and pulsed release. In Table 1, the external dimensions of both the ISO/ventilated containers and the IBCs are listed.

Table 1 External dimensions of the containers and IBCs

	Length [m]	Width [m]	Height [m]	Volume [m ³]	Area [m ²]
Container	5,9	2,35	2,4	33,28	13,87
IBC	1,2	1	1,016	1,22	1,2

The venting system is what changes in the two configurations of the containers. Figure 1 shows the geometrical differences between them.

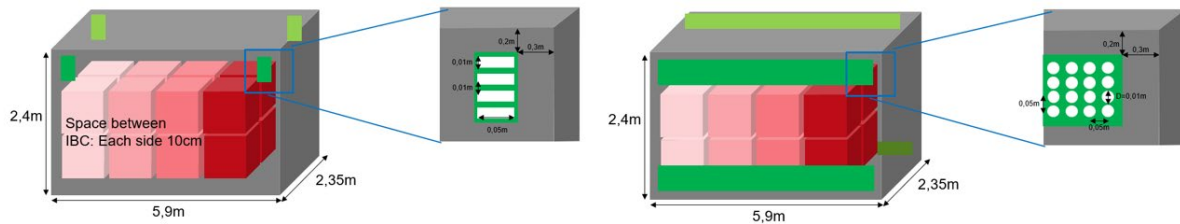


Figure 1 Venting system configurations: ISO container on the left; Coffee (ventilated) on the right.

When the type of release is continuous, the emitting rate is equal to the production of gas (this case refers the scenario in which safety valves are not used and the top lid of every IBC is always open). To reproduce the effect of the safety valves, the opening and closing overpressures of the valves are supposed, respectively, equal to 25kPa and 24kPa. The overpressure refers to the difference between the internal pressure of the IBC and the pressure within the free volume of the container. With this assumption, each opening takes place approximately every 330s for 1s and the valve releases all the hydrogen accumulated in the IBC when the valve is closed. With this model all the valves open at the same moment. Figure 2 shows the total mass of hydrogen released within the container in the first 1000s, and the time history of the overpressure within a single IBC.

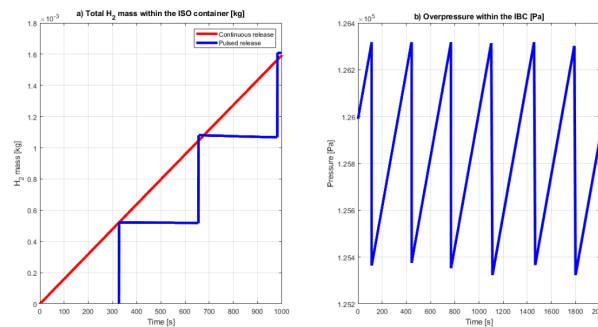


Figure 2 a) Total mass of hydrogen released within the container for the two types of release. b) Overpressure within the IBC.

In the simulations, two different mesh grids were used with different dimensions of the external environment. Inside the container, for both the mesh grids, every cell located far from the release points is a cube 10 cm wide, whereas the cells that are close to the release points are 5 cm wide. When external conditions of wind and sun are not considered, the external domain is extended of 1m on every axis. In the external environment the finest cell is on external wall and equal to the 10cm cube cells, and the following 5 cells have bigger dimension. When sun and wind are considered, external domain is extended of 10m on every axis. Table 2 summarizes the cells and the size of the two mesh grids.

Table 2 Dimensions and number of cells of the mesh grids.

External effects	Cells on x	Cells on y	Cells on z	Total cells	Domain
No	79	39	34	104754	7,9x4,3x3,4 m
Yes	99	59	54	315414	25,9x24,3x14,4m

Thirty measurement points were defined inside the containers to calculate the hydrogen concentration. Their placements are in the free spaces between the solid surfaces of the IBCs and the walls of the enclosure. There are fifteen points in the mid-height of the container, in the free space between the lower IBCs and the upper IBCs ($z=1,2$ m), and other fifteen sensors are located in the free gaps between the upper IBCs and the ceiling ($z=2,35$ m). Figure 3 shows the measurement points at $z=1,2$ m, and the yellow cells refer to the areas where the hydrogen is released. Both the lower and upper IBCs release gaseous hydrogen.

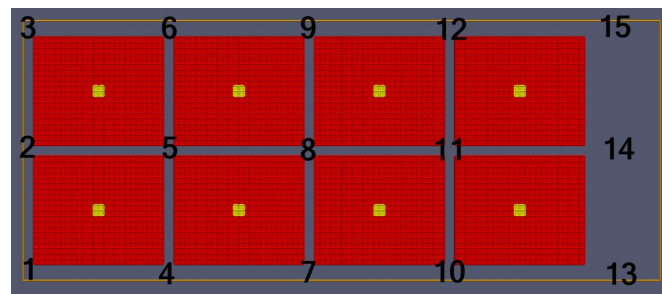


Figure 3 Placements of measuring points at $z=1,2$ m.

The boundary conditions applied were a mass flow inlet for the points of release, pressure outlet for the outflows, and a velocity boundary condition as velocity inlet to reproduce the wind. The pressure outlet is located on the top of the external boundary domain for all cases. In the wind driven ventilation scenario, symmetry boundaries were modelled also with a pressure outlet boundary condition, as well as the wind outflow boundary. Except for the scenario with the sun radiation, atmospheric temperature was supposed equal to 300 K because heat transfer is not considered in the process. Instead, when the sun radiation is considered, the atmospheric temperature is 294.15K and the hot wall temperature is 296.15K. The hot wall has a constant temperature on the external face, while at $t=0$ s the internal face has the same temperature of all the other walls (294,15K).

To accept the mesh grids, GASFLOW-MPI was validated with a study found in literature in which experimental data of helium release in a confined space are available [5], using a similar mesh grid. Results are qualitatively consistent with the experiments because a quasi-steady state is reached around 400s, and sensors below the vent have the same concentrations. Quantitatively, helium concentrations are higher than experimental data, as shown in Figure 4. As the simulations reproduce the process well at a qualitative level, and provide higher helium concentrations than the experimental data, making the results more cautious in terms of safety, the coarse mesh grid can be used for a conservative analysis.

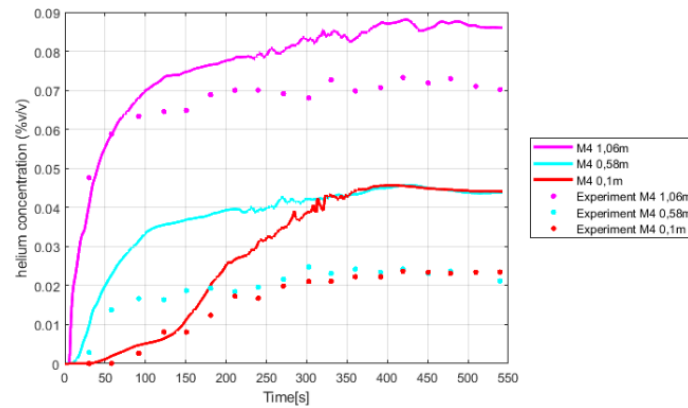


Figure 4 Comparison of the predicted helium concentration time histories and experimental ones at sensor M4.

In addition, a sensitivity analysis on the mesh grid for the case with continuous release and without external effects was tested doubling the number of cells on every axis. Simulation with refined mesh was performed for 10000s, and the hydrogen concentration at measurement points 8 ($z=1,2\text{m}$ and $z=2,25\text{m}$) were compared with those obtained with a coarse mesh. In Figure 5, the evolution in time of the concentrations of hydrogen of the two grids are plotted.

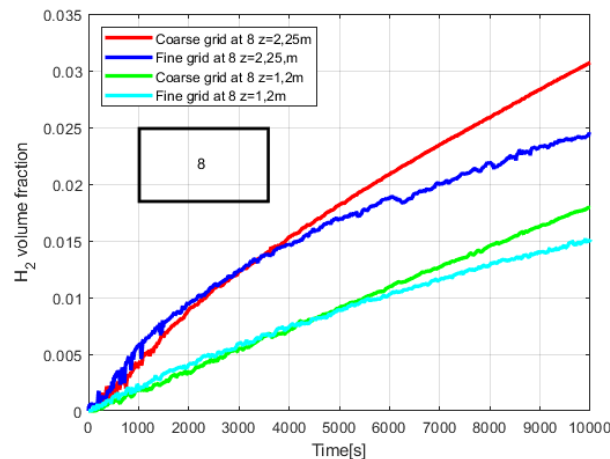


Figure 5 Mesh sensitivity for the continuous release case of the ISO container.

The velocities for a finer mesh are two times bigger than the coarse mesh, which means that buoyancy forces are stronger. The plumes raising from the lower IBCs impinge the ceiling first in the refined mesh case, and then the hydrogen spreads throughout the top of the enclosure. This explains why in the first stages ($\sim 3000\text{ s}$) the finer mesh has higher concentrations. Later, the most efficient ventilation due to the higher velocities, makes the hydrogen concentration lower than the coarse mesh grid. The sensitivity analysis on the grid showed that more conservative values were obtained with a less refined mesh.

The goal of this study is to understand which are the effects of safety valves, wind and sun on the concentration and distribution of hydrogen within the container compared with the reference case. Being the results with coarse grid cautionary compared with those with finer mesh, the analysis was done with a conservative approach. Generally, for enclosed spaces with ventilation it is recommended to prevent accumulation of hydrogen at concentrations even lower than LFL, but in this case LFL is considered the upper limit of acceptance.

4. RESULTS AND DISCUSSION

The reference case is an ISO container with continuous releases from all the 16 IBCs. Hydrogen, due to its density, raises into the container and hits the ceiling and propagates there. The hydrogen cloud formed is then pushed downward by the new hydrogen raising within the container. Over time hydrogen distribution becomes stratified, as shown in Figure 6.

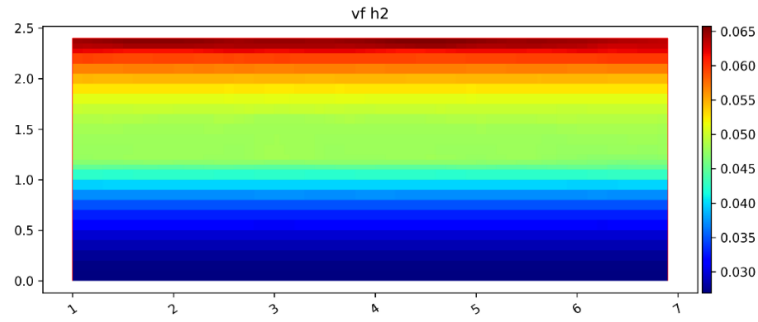


Figure 6 Hydrogen concentration contour (continuous releases) in the middle of the container (width $y=1,2m$) at 30000s.

As shown in Figure 7, the measurement points on the top reach the concentration LFL after approximately 15000s, while the points below reach LFL after approximately 24000 s.

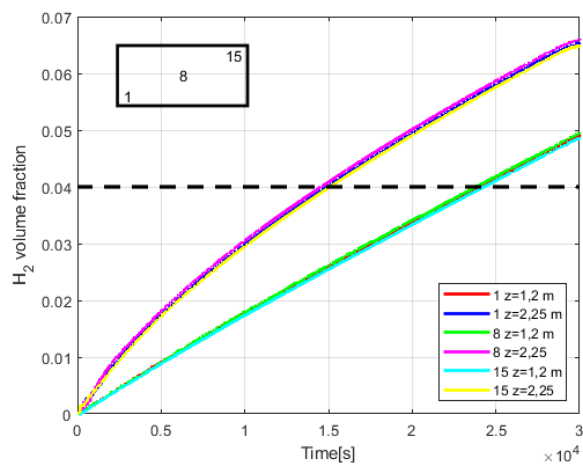


Figure 7 Time histories plot of the hydrogen concentrations at different heights (continuous releases).

The second scenario is an ISO container in which 16 IBCs provided with safety valves are located. The releases are pulsed. In this case, plumes are richer of hydrogen and faster than plumes in the reference case due to the higher velocities of the releases. At each opening, hydrogen rich clouds are created, and the mixing phenomena is enhanced by the inertia of the raising plumes. When the valves are closed, buoyancy forces become dominant, and stratification takes place. Hydrogen distribution is then influenced by the succession of these two phenomena, as shown in Figure 8.

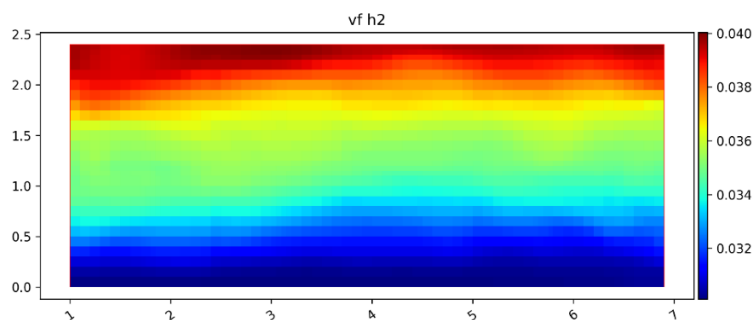


Figure 8 Hydrogen concentration contour (pulsed releases) in the middle of the container (width $y=1,2m$) at 30000s.

The safety valves have a positive effect on the process. Due to the higher velocities of the releases, there are two favourable results compared to the reference case: better mixing and better ventilation. Ventilation, however, is not enough to maintain the hydrogen concentration below the LFL. At the

measurement points on the top, LFL is reached around 30000s (Figure 9) and there is a delay of approximately 15000s compared to the continuous case.

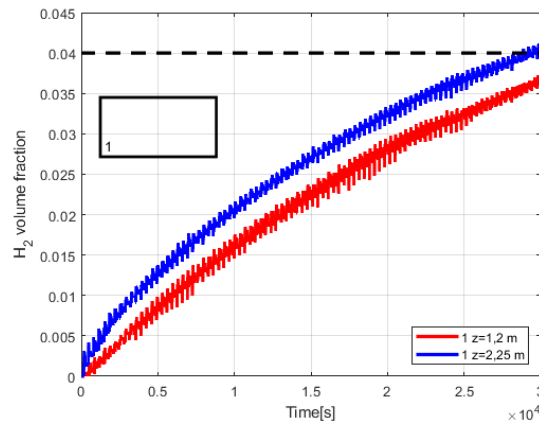


Figure 9 Time histories plot of the hydrogen concentrations at different heights (pulsed releases).

Wind was supposed directed straight to the vent with a magnitude of 1m/s. The wind entering from the upwind vents drives the air and hydrogen to the downwind vents. Thus, when hydrogen rich clouds raise to the ceiling, they are moved by the air coming from the windward wall. Some hydrogen is released outside while the remainder recirculates inside the container.

Concentration of hydrogen is after 10000s constantly below 1%, and concentration growth appears to be very weak after the first 4000s, as shown in Figure 10.

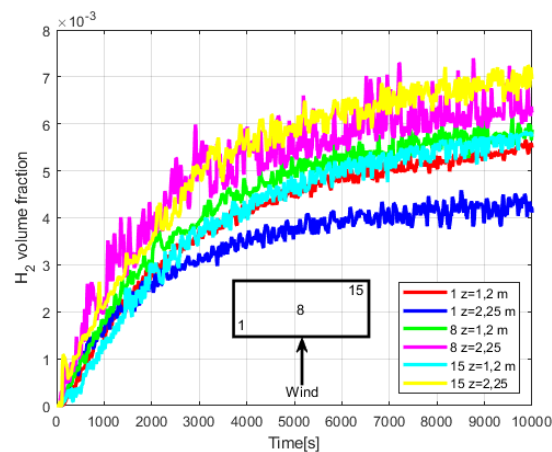


Figure 10 Time histories plot of the hydrogen concentrations at different heights (Wind driven ventilation).

When a wall is irradiated by the sun, its temperature increases. Supposing that the difference in temperature between the irradiated wall and the others is 2°C. The thickness of the walls is 20cm and the material is steel ($\rho=7850\text{kg/m}^3$; $c_p=492\text{J/kgK}$; $k=50\text{W/mK}$; $\alpha=1,3 \times 10^6\text{m}^2\text{s}$).

Convective motions are established from the hot wall to the cold walls. After the release, hydrogen raises up due to the buoyancy force. When it reaches the ceiling, it is pushed by the hot air to the cold wall due to the convective motion established by the difference in temperature. This circulation continues, and gradually hydrogen mixes with air. After 10000s, homogenization takes place, and difference in concentration is negligible between all the points within the container. as shown in Figure 11.

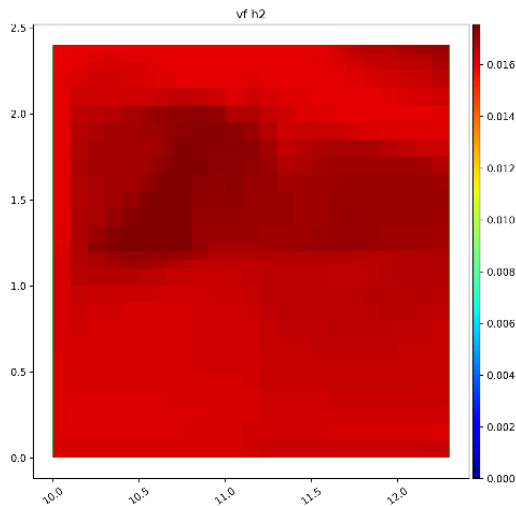


Figure 11 Hydrogen distribution contour in the middle of the ISO container for the sun radiation scenario ($x=5,5m, 10000s$).

After the first 1000s, the hydrogen concentration seems to increase linearly at all the points, and its values are very similar, as reported in Figure 12 (left). Simulation was carried out until 10000s to save computational time, but LFL is not reached. To calculate when it is reached, a linear model over time on the hydrogen concentration growth is assumed. In Figure 12 (right), a dashed line has been drawn to predict the time histories of this scenario up to 30000s. According to this model, LFL is reached around 24200s. Being the mixing strong, LFL could be reached in every point of the container at the same time.

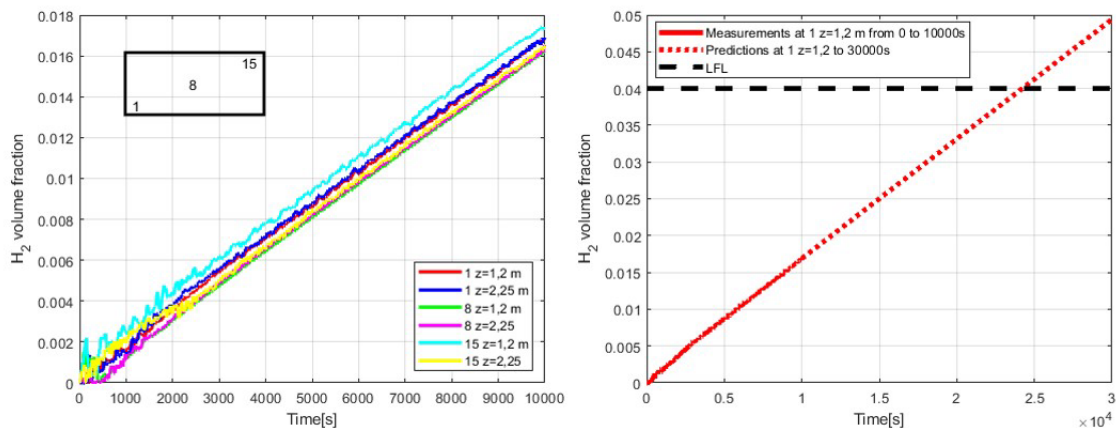


Figure 12 Time histories plot of the hydrogen concentrations at different heights on the left, and the linear model for evaluate the reaching of the LFL on the right. (sun radiation scenario)

The last simulation refers to a Coffee container with continuous releases of hydrogen from the IBCs. Steady state regime is reached around 5000s, and hydrogen is mostly accumulated on the top of the container, between the upper IBCs and the ceiling. In Figure 13, the time histories of the hydrogen concentration show that there is a big difference between the upper and lower measurement points.

The most efficient ventilation was reached thanks to both the bigger total area of the vents, and also to the openings on the bottom that helped the new fresh air flow in and the mixture of air and hydrogen escape from the vents on the top.

To evaluate the effective ventilation of all scenarios, the total mass vented outside from the container was also calculated. After a duration of 10,000 seconds, a total of 16 grams of hydrogen was released within the container. The corresponding values for the total masses of hydrogen released outside are presented in Table 3.

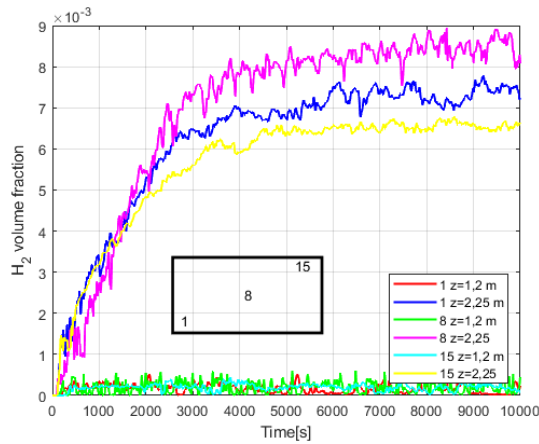


Figure 13 Time histories plot of the hydrogen concentrations at different heights (Coffee container).

Table 3 Total mass of hydrogen released in the external environment from the container after 10000s.

Case	1	2	3	4	5
H ₂ vented	0,43 g	1,6 g	11 g	0,38 g	14,5 g
	2,6%	10%	70%	2,3%	90%

5. CONCLUSIONS

In this study, a CFD analysis on hydrogen safety was carried out with GASFLOW-MPI CFD code. Releases of hydrogen took place in a 20ft container from 16 IBCs, and different scenario were considered. First, a continuous release in an ISO container was tested. Then, the release was investigated pulsed thanks to the safety valves model. Wind driven ventilation was evaluated. Later, also the effect of the sun radiation was studied. And lastly, the effect of a ventilated geometry of the container was checked.

The main results of all scenarios are listed below:

- Continuous release within the ISO container: the concentration of hydrogen results stratified, and the mixing between hydrogen and air is weak. The venting system is not able to avoid that flammable atmosphere is formed within the container, and LFL is reached on the top of the container after around four hours.
- Pulsed release within the ISO container: once again, the distribution of hydrogen is stratified, but less marked. Both mixing and venting are more efficient, but they are not able to avoid LFL within the container, that is reached after approximatively eight hours.
- Wind driven ventilation within the ISO container: the venting phenomena is very strong. It can push out the 70% of the hydrogen released from the IBCs. The results state that LFL is not reached in the simulation.
- Sun radiation on a wall of the container: A difference in temperature between the walls of the container was investigated. The result is a strong mixing without stratification. The convective motions created by the difference in temperature led to a homogenization of the mixture. The venting phenomena is weak. In fact, hydrogen concentration is lower than the first two cases only because the mixing is stronger, but, over time, it increases linearly and LFL is reached after around six hours and a half in all the points of the container.
- Continuous release within the Coffee container: the venting of hydrogen is very efficient. The 90% of the total hydrogen released from the IBCs is pushed out by the venting phenomena. Hydrogen is local accumulated on the top of the container and hydrogen concentration below is very low.

In a real case, the wind is variable in intensity and direction, and depends mainly on the place where the container is placed. The same can be said about solar radiation. Another scenario of interest could be studying more containers placed next to each other, or one above the other. The approach used in this analysis is conservative, and results might have a certain percentage of error in excess for the hydrogen concentration and total mass. Thus, this work can be used as a starting point for further investigation with more accuracy. The obtained results give the idea of what can happen, and what can be the effects of the safety valves, the wind, the sun, and different geometries of the container.

REFERENCES

- [1] Safety of Hydrogen as an Energy Carrier, [Online]. Available: www.hysafe.org.
- [2] InsHyde - Hydrogen Releases in Confined and Partially Confined Spaces, [Online]. Available: <http://www.hysafe.org/InsHyde>.
- [3] SUSANA Project, [Online]. Available: <https://www.h2fc-net.eu/collaboration/susana-database/>.
- [4] Hysafe, “Initial Guidance for Using Hydrogen in Confined - Results from InsHyde,” 30 January 2009. [Online]. Available: http://www.hysafe.org/download/1710/HYSAFE_D113_version_1.1.pdf.
- [5] S. G. Giannissi, V. Shentsov, D. Melideo, B. Cariteau, D. Baraldi, A. G. Venetsanos e V. Molkov, CFD benchmark on hydrogen release and dispersion in confined, naturally ventilated space with one vent, *International Journal of Hydrogen*, vol. 40, n. 5, pp. 2415-2429, 2015.
- [6] M. De Stefano, X. Rocourt, I. Sochet e N. Daudey, Hydrogen dispersion in a closed environment, *International Journal of Hydrogen Energy*, vol. 44, n. 17, pp. 9031-9040, 2019.
- [7] Operating Safety Committees of the Silicones Environmental, Health and Safety Center (SEHSC), CES-Silicones Europe (CES), “Materials Handling Guide: Hydrogen-Bonded Silicon Compounds,” July 2016. [Online]. Available: <https://www.dow.com/documents/en-us/sih-manual-revised-july-2016.pdf>.
- [8] J. Xiao, J. Travis, P. Royl, G. Necker, A. Svishchev e T. Jordan, *GASFLOW-MPI: A Scalable Computational Fluid Dynamics Code for Gases, Aerosols and Combustion. Theory and Computational Model*, vol. 1, Karlsruhe: KIT, 2011.
- [9] J. Xiao, J. Travis, P. Royl, G. Necker, A. Svishchev e J. Jordan, *GASFLOW-MPI: A Scalable Computational Fluid Dynamics Code for Gases, Aerosols and Combustion. Theory and Computational Model*, vol. 2, Karlsruhe: KIT.
- [10] P. R. Spalart, Detached-Eddy Simulation, *Annual Review of Fluid Mechanics*, vol. 41, n. 1, pp. 181-202, 2009.
- [11] P. R. Spalart, Strategies for turbulence modelling and simulations, *International Journal of Heat and Fluid Flow*, vol. 21, n. 3, pp. 252-263, 2000.
- [12] H. Zhang, H. Li, J. Xiao e T. Jordan, Detached Eddy Simulation of hydrogen turbulent dispersion in nuclear containment compartment using GASFLOW-MPI, *International Journal of Hydrogen Energy*, vol. 43, n. 29, p. 13659—13675, 2018.